Multimode effects in cavity QED based on a one-dimensional cavity array

Wei Zhu,[1] Z. H. Wang,[2] and D. L. Zhou[1,*]

[1]*Institute of Physics, Beijing National Laboratory for Condensed Matter Physics, Chinese Academy of Sciences, Beijing 100190, China*

[2]*Beijing Computational Science Research Center, Beijing 100084, China*

(Received 15 May 2014; published 16 October 2014)

We present a microscopic model of cavity quantum electrodynamics based on a one-dimensional (1D) coupled cavity array (CCA), where a supercavity (SC) is composed by a segment of the 1D CCA with relatively smaller couplings with the outsides. The single-photon scattering problem for the SC empty or with a two level atom in it is investigated. We obtain the exact theoretical result on the transmission rate for our system, which predicts that the transmission peaks shall appear near the eigenenergies of the SC. Our numerical results further prove that the SC is a well-defined multimode cavity. When a two level atom resonant with the SC locates at the antinode of the resonant mode, the transmission spectrum shows a clear sign of vacuum Rabi splitting as expected. However, when the atom locates at the node of the resonant mode, we observe a deep valley in the transmission peak, which can be explained by the destructive interference of two transmission channels: one is the resonant mode, while the other is arising from the atom coupling with the nonresonance modes. The effect of nonresonance modes on vacuum Rabi splitting is also analyzed.

DOI: 10.1103/PhysRevA.90.043828 PACS number(s): 42.50.Pq, 42.50.Gy, 32.80.Qk

I. INTRODUCTION

Cavity QED, the study of the interaction between atoms and the quantized electromagnetic fields in a microcavity, has been one of the central research areas in both quantum optics and quantum information since the pioneering work of Purcell [1]. In a single cavity with one atom or multiatoms, the hallmark phenomena, such as vacuum Rabi splitting [2], Rabi oscillation [3], collective Lamb shift [4], and electromagnetically induced transparency [5], have been successfully observed.

With the rapid development of experimental technologies in recent years, the system of a coupled cavity array (CCA) with atoms embedded in it has aroused significant attention. It is a promising test bed which is widely used in various areas and also a building block for important quantum devices. In quantum simulation, many important phenomena in condensed matter have been successfully observed on this platform, such as Mott-superfluid transitions [6–8] and some topological effects [9–12].

A CCA also shows its application in controlling single photons, which is of essential importance in quantum optics and quantum information. One of the pioneering works [13] focuses on a one-dimensional (1D) CCA doped with a two level system and shows that the controllable system can behave as a quantum switch for the coherent transport of single photon. Furthermore, the single-photon scattering for a 1D CCA with a pair of two level atoms or with three level atoms has also been discussed [14]. Aside from the 1D CCA, single-photon scattering for a two-dimensional CCA is also important for its promising application in quantum networks [15]. In addition, a CCA may be introduced in more research areas; e.g., a recent paper designed an experiment on a CCA to explore the basic principle in quantum mechanics [16].

In this paper, we use a CCA to investigate the basic problem in cavity QED. Based on a 1D CCA, we propose a new real space cavity model with a supercavity (SC) as our cavity. The characteristics of a SC empty or with a two level atom doped in it are explored by studying the single-photon scattering problem. Applying the discrete coordination scattering equation [13] to the case of an empty SC, we give the transmission spectrum in order to numerically and analytically prove that the transmission peaks shall appear near the eigenvalues of the empty SC system. These transmission peaks with nonzero width imply that the empty SC can be considered as a well-defined multimode cavity with dissipation.

In particular, we consider the variation of the single-photon transmission due to a two level atom which is near resonant with one of the SC modes. When the atom is located at the antinode of the resonant mode, we observe the vacuum Rabi splitting in the transmission spectrum. However, when the two level atom is located at the node of the resonant mode, i.e., it does not interact with the resonant mode, an obvious valley in the transmission spectrum is observed, which is further explained by the destructive interference of two transmission channels: one is provided by the resonant mode of the SC, while the other results from the two level atom which couples to the nonresonance modes of the SC.

The rest of the paper is organized as follows. In Sec. II, we introduce the theoretical model of our system and give the analytical result of the single-photon transmission rate. In Sec. III, we study the single-photon scattering on the empty SC, which shows the characteristic features of the SC. In Sec. IV, we investigate in detail how a two level atom essentially changes the transmission spectrum, especially focusing on the effect of nonresonance modes of the SC. In Sec. V, we introduce the two level approximation of the SC system to physically explain the transmission valley as the destructive interference between the two transmission channels assisted by the two levels, respectively. In Sec. VI, we briefly discuss the experimental feasibility of the theoretical predictions and give a summary of our results.

II. MODEL AND THEORETICAL RESULTS

The system we consider is composed by a two level atom interacting with the nth cavity in a 1D coupled single mode

*zhoudl72@iphy.ac.cn

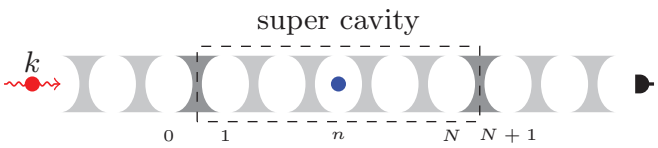

FIG. 1. (Color online) Schematic configuration of the single-photon scattering problem for the 1D CCA model. A single photon (filled red circle) with the wave vector k injects from the left side of the supercavity composed of N cavities, which is formed by a relatively small coupling strength η with the outside cavities. A two level atom (filled blue circle) is in the nth cavity of the SC. The transmission spectrum is measured by the detector on the right side of the SC. Here we take $N = 5$ and $n = 3$.

cavity array with infinite length, which is shown in Fig. 1. The hopping strength between neighboring cavities l and $l+1$ is ξ for $l \notin \{0,N\}$, and the hopping strength is η for $l \in \{0,N\}$, which is much less than ξ. In such a setting, the cavities between 1 and N form a secondary cavity, which we will call the supercavity hereafter. Meanwhile, the two level atom is required to be inside the supercavity, i.e., $1 \leqslant n \leqslant N$.

A tight-bonding model including five parts is introduced to describe the system

$$H = H_S + H_L + H_R + H_{SL} + H_{SR}, \tag{1}$$

where

$$H_S = \sum_{j=1}^{N} \omega_c a_j^\dagger a_j + \sum_{j=2}^{N} \xi (a_{j-1}^\dagger a_j + a_j^\dagger a_{j-1}) + \omega_a |e\rangle\langle e| + g(a_n^\dagger \sigma^- + \text{H.c.}), \tag{2}$$

$$H_L = \sum_{j=-\infty}^{0} [\omega_c a_j^\dagger a_j + \xi (a_{j-1}^\dagger a_j + a_j^\dagger a_{j-1})], \tag{3}$$

$$H_R = \sum_{j=N+1}^{\infty} [\omega_c a_j^\dagger a_j + \xi (a_j^\dagger a_{j+1} + a_j^\dagger a_{j+1})], \tag{4}$$

$$H_{SL} = \eta (a_0^\dagger a_1 + \text{H.c.}), \tag{5}$$

$$H_{SR} = \eta (a_N^\dagger a_{N+1} + \text{H.c.}). \tag{6}$$

Here H_S describes the SC system, H_L (H_R) describes the left (right) channel that is formed by the segment of the cavity array left (right) of the SC, and H_{SL} (H_{SR}) describes the interaction between the SC with the outsides. $a_j^\dagger$ (a_j) is the photon creation (annihilation) operator for the jth single mode cavity, $|e\rangle$ ($|g\rangle$) is the excited (ground) state of the atom, and $\sigma^-(\sigma^+)$ is the atomic lowering (raising) operator. ω_c is the intrinsic frequency of each single mode cavity, ω_a is the transition frequency of the two level atom, and g is the coupling strength between the cavity and the atom. ξ is the coupling strength between neighboring cavities in the SC, the left channel and the right channel, while η is the coupling strength of neighboring cavities between them. In addition, we require that $\eta \ll \xi$ and set $\hbar = 1$ throughout this paper.

The basic task here is to investigate the single-photon scattering problem. When a single photon with wave vector k injects from the left channel toward the SC system, what is the transmission spectrum obtained in the right channel?

Now the scattering state can be expanded as

$$|\Psi_k\rangle = |\phi_k\rangle + r|\phi_k^*\rangle + t|\vartheta_k\rangle + \sum_{j=1}^{N} d_j|j\rangle + \lambda|e\rangle, \tag{7}$$

where

$$|\phi_k\rangle = \sum_{j=-\infty}^{0} e^{ikj}|j\rangle, \tag{8}$$

$$|\vartheta_k\rangle = \sum_{j=N+1}^{+\infty} e^{ikj}|j\rangle, \tag{9}$$

with $|j\rangle = a_j^\dagger|G\rangle$ and $|e\rangle = \sigma^+|G\rangle$. Here, $|G\rangle = |\text{vac}; g\rangle$ represents the state with all the cavities in their vacuum states while the atom is in the ground state. In Eq. (7), the coefficients r and t are the reflection and transmission amplitudes, respectively; d_j is the probability amplitude for finding the photon in the jth cavity; and λ is the probability amplitude for the atom in the excited state. The scattering state satisfies the stationary Schrödinger equation:

$$H|\Psi_k\rangle = E_k|\Psi_k\rangle. \tag{10}$$

In general, the transmission amplitude t is completely determined by Eq. (10), and the transmission rate $T = |t|^2$ can be obtained. One of our main theoretical results is

$$t = \frac{ie^{-i(k+\pi)(N+1)}2\gamma^2 \sin k}{e^{-2ik}|A_N^n| + \gamma^2 e^{-ik}\left(|A_{N-1}^n| + |A_{N-1}^{n-1}|\right) + \gamma^4 |A_{N-2}^n|}, \tag{11}$$

where $\gamma = \eta/\xi$ and $A_N^n = [H_S(N,n) - E_k]/\xi$ with the dispersion relation $E_k = \omega_c + 2\xi\cos k$ (the wave vector k is dimensionless by setting the distance between two arbitrary neighboring cavities as the unit), $H_S(N,n)$ is the Hamiltonian of the SC system with N cavities and the two level atom in the nth cavity, and $|A_N^n|$ is the determinant of A_N^n. The detailed derivation of Eq. (11) is given in the Appendix.

Since γ is a small parameter, the transmission peaks occur only when $|A_N^n|$ is small at least in the order of γ^2. In addition, $|A_N^n| = 0$ only when E_k is the eigenenergy of the SC system. Therefore, the necessary condition to observe the transmission peaks is that E_k is near resonant with the eigenmodes of the SC system.

III. SINGLE-PHOTON SCATTERING WITH EMPTY SUPERCAVITY

As the first step, we study the transmission spectrum for the SC without the two level atom, i.e., an empty SC. As is well known, the eigenvalues and eigenstates of the empty SC are

$$\nu_m = \omega_c + 2\xi\cos\theta_m, \tag{12}$$

$$|\Phi_m\rangle = \sqrt{\frac{2}{N+1}} \sum_{j=1}^{N} \sin(j\theta_m)|j\rangle, \tag{13}$$

where $\theta_m = \frac{m\pi}{N+1}$, with m being any integer between 1 and N.

Then the peaks in the transmission spectrum shall appear near the resonance $E_k = \nu_m$, i.e., $k = \theta_m$, which is numerically

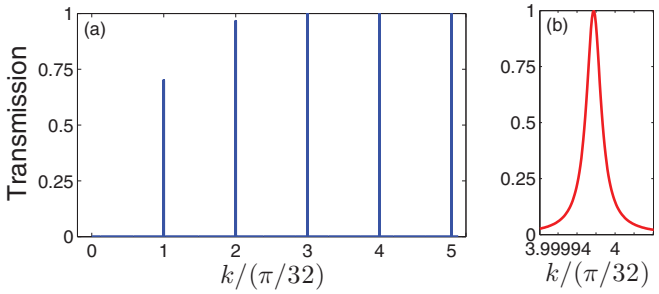

FIG. 2. (Color online) (a) The transmission rate vs the incident wave vector k for the empty SC. Only the first five transmission peaks are shown. (b) Zoom in of the fourth transmission peak. Here we choose the parameters $N = 31$, $\xi = 1$, and $\eta = 0.01$.

demonstrated in Fig. 2(a). In the figure, we only show the first five peaks, where the fourth peak is zoomed in in Fig. 2(b). It is apparent that each peak has a nonzero width, which means the corresponding electromagnetic mode in the SC system has a finite lifetime due to the dissipation arising from the coupling with the left and right channels. In other words, the left and right channels act not only as the carriers of the scattering waves but also as the dissipation reservoirs of the SC.

As demonstrated above, the numerical results show that the SC is essentially an N-mode cavity, and every eigenmode of the SC has a relatively long lifetime. In what follows, we will study how a single two level atom that couples with the SC can dramatically change the transmission spectrum, and we will investigate the effects induced by the multimode cavity fields.

IV. SINGLE-PHOTON SCATTERING WITH ONE ATOM IN THE SUPERCAVITY

When a two level atom interacts with the nth cavity, it is convenient to rewrite the Hamiltonian H_S in the eigenmodes of the SC as

$$H_S = \sum_k \nu_k b_k^\dagger b_k + \omega_a |e\rangle\langle e| + \sum_k g_k (b_k^\dagger \sigma_- + b_k \sigma_+), \quad (14)$$

where

$$b_k^\dagger = \sqrt{\frac{2}{N+1}} \sum_{j=1}^{N} \sin(j\theta_k) a_j^\dagger, \quad (15)$$

$$g_k = g\sqrt{\frac{2}{N+1}} \sin(j\theta_k). \quad (16)$$

Note that the coupling strength g_k depends on the location of the atom and the length of the SC. It is the standard model of cavity QED in the multimode setting.

When the frequency of the atom is near resonant with a preselection k^*th mode of the SC, we may adopt the single mode approximation for the SC. Then the two relative eigenenergy levels are

$$E_{k\pm} = \frac{\nu_{k^*} + \omega_a}{2} \pm \frac{\Delta_{k^*}}{2}, \quad (17)$$

where the vacuum Rabi splitting is

$$\Delta_{k^*} = \sqrt{(\nu_{k^*} - \omega_a)^2 + 4g_{k^*}^2}. \quad (18)$$

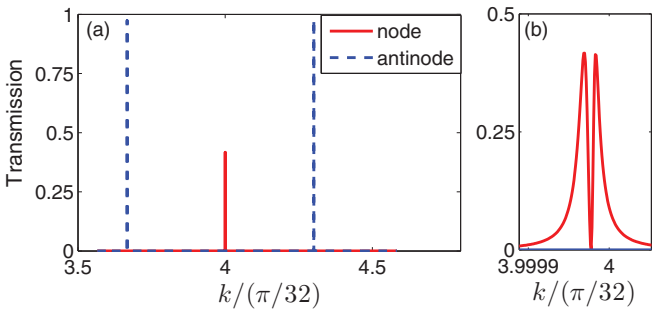

FIG. 3. (Color online) (a) Transmission rates vs the incident wave vector (just around the resonant mode). Blue dashed and red solid lines each stand for the atom at the antinode ($n = 12$) or node ($n = 8$) of the mode. (b) Zoom in of the red peak. Here the atom is near resonant with the fourth mode of the SC with $\omega_a = 1.847760755\xi$, and $g = 0.1$.

Now we numerically check the validness of the above single-mode approximation. First, we plot the transmission spectrum when the two level atom is located at the node and antinode of the resonant mode of the SC, which is shown in Fig. 3 (a). When the atom is located at the antinode of the resonant mode, the obvious vacuum Rabi splitting appears. When the atom is located at the node, i.e., the two level atom does not interact with the resonant mode of the SC, no vacuum Rabi splitting is observed as expected. However, the peak is lower than $1/2$ in the latter case. If the single mode approximation is valid, then the two level atom without interacting with the resonant mode of the SC will not affect the transmission rate. In other words, it is expected to be similar to the case shown in Fig. 2(b). Thus we plot the zoom in for the case of the atom at the node as shown in Fig. 3(b). Obviously, the transmission spectrum shown in Fig. 2(b) exhibits an obvious valley exactly at the resonant mode of the SC, which is essentially different from Fig. 7(b).

To investigate the physics underlying the transmission spectrum shown in Fig. 3(b), the frequency of the atom is tuned to be resonant with the mode while keeping the atom at the node, and the transmission spectrum is given for different coupling strengths g as shown in Fig. 4(a). When $g = 0$, we recover the transmission spectrum shown in Fig. 2(b). When g is not equal to zero, a second peak appears near the frequency of the atom. Since the atom does not couple with the resonant mode, the peak must be originated from the atom coupling with

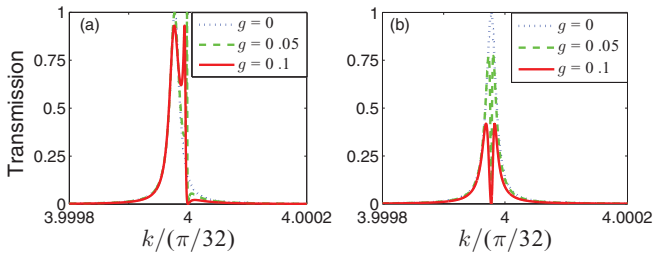

FIG. 4. (Color online) Transmission spectrum for the atom at the node of the resonant mode with $g = 0$ (blue dotted line), $g = 0.05$ (green dashed line), and $g = 0.1$ (red solid line). (a) $\omega_a = \nu_4$. (b) $\omega_a = 1.847760755\xi$.

the nonresonance modes. We assert that due to the different influences of the outsides the transmission spectrum for each channel independently partially overlaps at the resonant condition, which leads to the above-mentioned transmission spectrum as shown in the next section. By increasing g, the transmission peak becomes wider as expected. The numerical result in Fig. 4(a) clearly shows that in the case of the atom located at the node of the resonant mode two channels exist for the photon transmitting through the SC: one is the resonant cavity, while the other results from the atom coupling with the nonresonance modes.

Further, as shown in Fig. 4(b), we tune the frequency of the atom so that the transmission peaks for the two channels coincide as shown in the next section. However, we find that the single photon is completely reflected at the original transmission peak of the resonant mode, which implies that the transmission amplitudes through the two channels interfere destructively. The appearance of the transmission valley comes from the different widths of the transmission peaks from the two channels. Moreover, the widths of the valleys are determined by the coupling strength g, which further confirms the existence of quantum interference. A more physical explanation of the transmission spectrum is given in the next section to intuitively show the mechanism behind the transmission dip.

As discussed above, the nonresonance modes dramatically change the transmission spectrum when the atom is located at the node, so a natural problem is how the nonresonance modes affect the transmission spectrum when the two level atom is located at the antinode of the resonant mode. To this end, we plot the transmission spectrum for different detunings when the atom is located at the antinode as shown in Fig. 5. We show that, by tuning the frequency of the atom higher than the resonant mode, the peak of the high frequency will move away faster than the one with the low frequency, and the opposite behavior can be seen if tuning the atom frequency lower. Obviously, this behavior cannot be explained by the single mode approximation and must be attributed to the effects of nonresonance modes of the SC. Notice that a similar phenomenon is mentioned in [17].

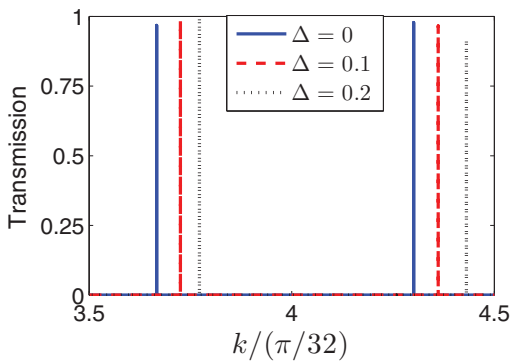

FIG. 5. (Color online) Transmission spectrum for different detunings when the atom is located in the antinode. Here we give the results for $\Delta = \omega_a - \nu_4 = 0$ (blue solid line), $\Delta = 0.01\xi$ (red dashed line), and $\Delta = 0.02\xi$ (black dotted line).

V. PHYSICAL EXPLANATION OF THE TRANSMISSION VALLEY IN THE TWO LEVEL APPROXIMATION

Now let us give a more detailed and physical explanation about the transmission valley shown in Fig. 4. As we know, the energy levels of the SC that are near resonant with the energy of the incoming photon dominate the photon transmission through the SC. In the cases that the transmission valley occurs, there are two energy levels of the SC that are near resonant with the energy of the incoming photon: one is the near resonant mode of the SC that does not interact with the atom, and the other is the atomic excited state dressed by the nonresonance modes. Thus it is reasonable to maintain only these two levels in the Hamiltonian H_S, which is called the two level approximation. In the two level approximation, the Hamiltonian of our system can be written as $H = H_S + H_L + H_R + H_{SL} + H_{SR}$, with H_L and H_R the same as in the exact model and

$$H_S = \nu_m|\psi_m\rangle\langle\psi_m| + \omega_A|\varphi_m\rangle\langle\varphi_m|, \tag{19}$$

$$H_{SL} = \eta\left[(\alpha_1|0\rangle\langle\psi_m| + \beta_1|0\rangle\langle\varphi_m|) + \text{H.c.}\right], \tag{20}$$

$$H_{SR} = \eta\left[(\alpha_2|N+1\rangle\langle\psi_m| + \beta_2|N+1\rangle\langle\varphi_m|) + \text{H.c.}\right], \tag{21}$$

where $|\psi_m\rangle = b_m^\dagger|G\rangle\alpha_1 = \langle 1|\psi_m\rangle$, $\beta_1 = \langle 1|\varphi_m\rangle$, $\alpha_2 = \langle N|\psi_m\rangle$, and $\beta_2 = \langle N|\varphi_m\rangle$. ω_A is the eigenenergy of the atomic state.

Now the scattering state can be expanded as

$$|\Psi_k\rangle = |\varphi_k\rangle + r|\varphi_k^*\rangle + t|\vartheta_k\rangle + \mu|\psi_m\rangle + \zeta|\varphi_m\rangle, \tag{22}$$

with μ and ζ being the excitation amplitudes of the modes $|\psi_m\rangle$ and $|\varphi_m\rangle$, respectively.

The stationary Schrödinger equation $H|\Psi_k\rangle = E_k|\Psi_k\rangle$ results in the following set of scattering equations:

$$\omega_c r' + \xi(e^{-ik} + re^{ik}) + \eta(\alpha_1\mu + \beta_1\zeta) = E_k r', \tag{23}$$

$$\eta[r'\alpha_1 + t'\alpha_2] + \nu_m\mu = E_k\mu, \tag{24}$$

$$\eta[r'\beta_1 + t'\beta_2] + \omega_A\zeta = E_k\zeta, \tag{25}$$

$$\omega_c t' + \eta(\alpha_2\mu + \beta_2\zeta) + \xi t' e^{ik} = E_k t', \tag{26}$$

and the transmission rate $T = |t|^2$ can be determined. Here, we set $t' = te^{ik(N+1)}$ and $r' = 1 + r$.

From Eq. (26), the condition for the perfect reflection is

$$\alpha_2\mu + \beta_2\nu = 0. \tag{27}$$

Equation (27) can be understood as follows. When the three levels $|\psi_m\rangle$, $|\varphi_m\rangle$, and $|N+1\rangle$ are considered, the state $\mu|\psi_m\rangle + \zeta|\varphi_m\rangle$ is the dark state relative to $|N+1\rangle$ as in the electromagnetically induced transparency setting. This shows the interference mechanism behind the transmission valley and is the central point to understand the phenomenon.

A. Analytical and numerical results for $\omega_a = \nu_m$

When the atom is resonant with the mth mode of the cavity ($\omega_a = \nu_m$), the state $|\varphi_m\rangle$ with eigenenergy $\omega_A = \omega_a$ can be

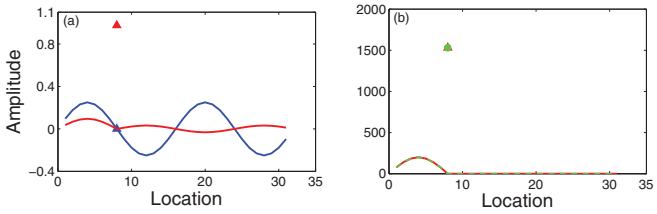

FIG. 6. (Color online) (a) The blue (red) solid line and triangle each represent the excitation amplitude of the SC and the atom as in state $|\psi_m\rangle$ ($|\varphi_m\rangle$). (b) The green dashed (red solid) line and triangle (circle) each represent the excitation amplitude of the SC and the atom as in state $|\Psi_m\rangle_{\rm SC}$ in the two level approximation model (the exact model). Here, $g = 0.05$ and $m = 4$ while all the other parameters are the same as before.

analytically expressed as

$$|\varphi_m\rangle = c_m^\dagger|G\rangle + d_m^\dagger|G\rangle - \frac{1+\gamma}{g\sqrt{A}}\sin\theta_m|e\rangle, \tag{28}$$

where

$$c_m^\dagger = \frac{1}{\sqrt{A}}\sum_{j=1}^{n}\sin(j\theta_m)a_j^\dagger,$$

$$d_m^\dagger = -\frac{\gamma}{\sqrt{A}}\sum_{j=n+1}^{N}\sin(j\theta_m)a_j^\dagger,$$

$$\gamma = n/(N-n+1),$$

$$A = \sqrt{\frac{N+1}{N-n+1}\left[\frac{n}{2} + \frac{N+1}{g^2(N-n+1)}\sin^2\theta_m\right]}.$$

The states $|\psi_m\rangle$ and $|\varphi_m\rangle$ are demonstrated in Fig. 6(a). In addition, a simple calculation shows that the perfect reflection appears at $E_k = \nu_m$. Then the analytical result of the scattering state within the SC

$$|\Psi_m\rangle_{\rm SC} = C\left[\sqrt{\frac{2}{N+1}}\sin(N\theta_m)c_m^\dagger|G\rangle + \frac{\alpha_2\sin\theta_m}{g\sqrt{A}}|e\rangle\right], \tag{29}$$

where

$$C = -\frac{2i(\gamma+1)\sin\theta_m}{\eta(\alpha_1\beta_2 - \alpha_2\beta_1)}.$$

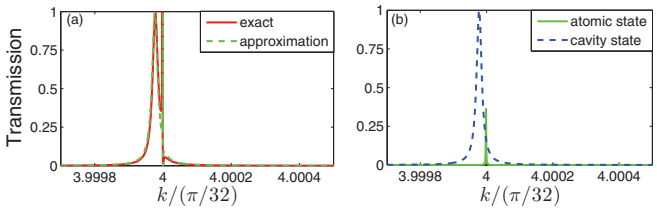

FIG. 7. (Color online) Transmission rates vs the incident wave vector for different models. (a) The results under the full Hamiltonian (red solid line) and two level approximation (green dashed line). (b) The results when we only consider one channel which is supported by the mth eigenstate of the SC (blue dashed line) and the atomic state (green solid line).

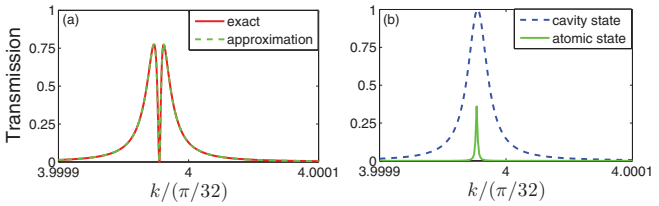

FIG. 8. (Color online) Transmission spectrum for various channels. The transition frequency of the atom $\omega_a = 1.847760755\xi$. (a) Blue dashed line: the cavity state $|\psi_m\rangle$. Green solid line: the atomic state $|\varphi_m\rangle$. (b) Green dashed line: the two level approximation. Red solid line: the exact model.

The state is clearly localized between the atom and the left end of SC, while the two modes represented by $|\psi_m\rangle$ and $|\varphi_m\rangle$ are extended throughout the SC (as clearly shown in Fig. 6).

To test the validness of the two level approximation, we compare the numerical results in the approximation with those from the exact model. As shown in Fig. 7(a), the transmission spectrum from the two level approximation agrees well with those from the exact model, which verifies that the transmission valley is a two level effect. To further clarify the two level approximation, we give the transmission spectrum when either one of the two levels is considered, which is shown in Fig. 7(b). Obviously, the transmission valley appears only in the overlap region due to quantum interference.

B. Numerical results for $\omega_a \neq \nu_m$

When the atom is near resonant with the mth mode of the SC, the analytical expression for the state $|\varphi_m\rangle$ is difficult to obtain. Then we numerically evaluate the state $|\varphi_m\rangle$ and the eigenenergy ω_A. The transmission spectrum within the two level approximation is shown in Fig. 8(a). As before, we also compare these approximate results with those from the exact model and find that the approximation is quite accurate. The transmission spectra from both of the two levels are shown in Fig. 8(b), which verifies that the transmission valley comes from the quantum interference between the two channels assisted by the two levels.

VI. REMARKS AND CONCLUSION

In this paper, we have studied the single-photon scattering in a typical CCA system. Experimentally, the CCA can be realized by the superconducting transmission line resonators which support the single mode microwave electromagnetic field with the resonant frequency $\omega_c/2\pi \approx 3$ GHz [18]. The coupling between neighboring resonators can be realized via the tunable capacitances and achieves strengths of $\xi(\eta)/2\pi =$ 5–100 MHz [18,19]. Correspondingly, the two level atom can be realized by a superconducting qubit such as the flux qubit whose transition frequency can be tuned by readily adjusting the flux through the loop, and a coupling strength of $g \approx 0.12\omega_c$ between the qubit and the resonator was achieved in a recent experimental scheme [20].

In conclusion, we propose a simple microscopic model of cavity QED based on a CCA and prove that the transmission peaks shall appear near the eigenvalues of the whole SC

system. One of the advantages of this model is that it provides a platform to deal with the nonresonance modes in the microscopic level. First we show that the SC composed by a segment of a 1D cavity array is a multimode cavity by studying the transmission spectrum through an empty SC. Then we study the multimode effects in the SC system by investigating the transmission spectrum for the SC interacting with a two level atom, located at the antinode or node of a preselected resonant mode of the SC. When the atom locates at the antinode, we observe the vacuum Rabi splitting in the transmission spectrum as expected. However, when the two level atom locates at the node of the near resonant mode, we find a valley in the transmission spectrum, which can be explained by the interference of the transmission amplitude through two channels: one channel is the resonant mode, and the other is the atomic excited state dressed by the nonresonance modes. We hope this model can enlighten the study of multimode effects in cavity QED.

ACKNOWLEDGMENTS

This work is supported by NSF of China (Grant No. 11175247) and National Key Basic Research Special Foundation of China (Grants No. 2012CB922104 and No. 2014CB921202). Z. H. Wang is supported by the China postdoctoral Science Foundation (under Grant No. 2014M560879).

APPENDIX: LOCATIONS OF THE PEAKS

By comparing the coefficients of $\{|j\rangle\}$ and $|e\rangle$ in the stationary scattering equation (10), we obtain

$$E_k = \omega_c + 2\xi\cos k, \tag{A1}$$

and

$$\omega_c r' + \xi(e^{-ik} + re^{ik}) + \eta d_1 = E_k r', \tag{A2}$$

$$\omega_c d_1 + \eta r' + \xi d_2 = E_k d_1, \tag{A3}$$

$$\omega_c d_j + \xi(d_{j-1} + d_{j+1}) = E_k d_j, \tag{A4}$$

$$\omega_c d_n + \xi(d_{n-1} + d_{n+1}) + \lambda g = E_k d_n, \tag{A5}$$

$$\lambda\omega_a + g d_n = \lambda E_k, \tag{A6}$$

$$\omega_c d_N + \xi d_{N-1} + t'\eta = E_k d_N, \tag{A7}$$

$$\omega_c t' + \eta d_N + \xi t' e^{ik} = E_k t'. \tag{A8}$$

where $2 \leqslant j \leqslant N-1$ and $j \neq n$.

For $\omega_a \neq E_k$, Eq. (A6) leads to

$$\lambda = \frac{g}{E_k - \omega_a} d_n. \tag{A9}$$

Substituting Eq. (A9) into Eq. (A5), we have

$$\left(\omega_c + \frac{g^2}{E_k - \omega_a}\right) d_n + \xi(d_{n-1} + d_{n+1}) = E_k d_n. \tag{A10}$$

We introduce the following parameters:

$$d_0 = 1 + r, \tag{A11}$$

$$d_{N+1} = te^{ik(N+1)}, \tag{A12}$$

$$\alpha = \frac{\omega_c - E_k}{\xi} = -e^{ik} - e^{-ik}, \tag{A13}$$

$$\beta = \frac{\omega_c - E_k + \frac{g^2}{E_k - \omega_a}}{\xi} = \alpha + \frac{g^2}{\xi(E_k - \omega_a)}, \tag{A14}$$

$$\gamma = \frac{\eta}{\xi}, \tag{A15}$$

$$\delta = e^{ik} - e^{-ik}. \tag{A16}$$

Then the scattering equation can be expressed in the following matrix form:

$$\begin{pmatrix}
\alpha + e^{ik} & \gamma & & & & & & & & & \\
\gamma & \alpha & 1 & & & & & & & & \\
 & 1 & \alpha & 1 & & & & & & & \\
 & & & \ddots & & & & & & & \\
 & & & 1 & \alpha & 1 & & & & & \\
 & & & & 1 & \beta & 1 & & & & \\
 & & & & & 1 & \alpha & 1 & & & \\
 & & & & & & & \ddots & & & \\
 & & & & & & & 1 & \alpha & 1 & \\
 & & & & & & & & 1 & \alpha & \gamma \\
 & & & & & & & & & \gamma & \alpha + e^{ik}
\end{pmatrix}
\begin{pmatrix} d_0 \\ d_1 \\ d_2 \\ \vdots \\ d_{n-1} \\ d_n \\ d_{n+1} \\ \vdots \\ d_{N-1} \\ d_N \\ d_{N+1} \end{pmatrix}
= \begin{pmatrix} \delta \\ 0 \\ 0 \\ \vdots \\ 0 \\ 0 \\ 0 \\ \vdots \\ 0 \\ 0 \\ 0 \end{pmatrix}, \tag{A17}$$

which is abbreviated as

$$BD = \Gamma, \tag{A18}$$

with

$$B = \begin{pmatrix} \alpha + e^{ik} & \gamma & \\ \gamma & A_N^n & \gamma \\ & \gamma & \alpha + e^{ik} \end{pmatrix} \tag{A19}$$

and

$$A_N^n = \frac{H_S - E_k}{\xi}. \tag{A20}$$

By applying Cramer's Rule, the transmission amplitude is

$$t = e^{-ik(N+1)} d_{N+1} = e^{-i(k+\pi)(N+1)} \frac{\delta \gamma^2}{|B|}, \tag{A21}$$

with $|B|$ the determinant of the matrix. From Eq. (A19), $|B|$ can be analytical expressed as

$$|B| = e^{-2ik} \left|A_N^n\right| + e^{-ik} \gamma^2 \left(\left|A_{N-1}^{n-1}\right| + \left|A_{N-1}^n\right|\right) + \gamma^4 \left|A_{N-2}^{n-1}\right|. \tag{A22}$$

As mentioned before, $\eta \ll \xi$ leads to $\gamma \ll 1$. Thus, in order to gain large transmission probability, $|A_N^n|$ in the denominator of Eq. (A22) must be small at least in the order of γ^2, which clearly shows that the transmission peaks should be achieved only near the eigenvalues of the SC system. This result is easy to generalize to a multiatom situation.

[1] E. M. Purcell, Phys. Rev. **69**, 681 (1946).
[2] R. J. Thompson, G. Rempe, and H. J. Kimble, Phys. Rev. Lett. **68**, 1132 (1992).
[3] M. Brune, F. Schmidt-Kaler, A. Maali, J. Dreyer, E. Hagley, J. M. Raimond, and S. Haroche, Phys. Rev. Lett. **76**, 1800 (1996).
[4] R. Rölsberger, K. Schlage, B. Sahoo, S. Couet, and R. Röfer, Science **328**, 1248 (2010).
[5] M. Mücke, E. Figueroa, J. Bochmann, C. Hahn, K. Murr, S. Ritter, C. J. Villas-Boas, and G. Rempe, Nature (London) **465**, 755 (2010).
[6] D. G. Angelakis, M. F. Santos, and S. Bose, Phys. Rev. A **76**, 031805(R) (2007).
[7] M. J. Hartmann, F. G. S. L. Brandaõ, and M. B. Plenio, Nat. Phys. **2**, 849 (2006).
[8] A. D. Greentree, C. Tahan, J. H. Coleand, and L. C. L. Hollenberg, Nat. Phys. **2**, 856 (2006).
[9] A. Kay and D. G. Angelakis, Europhys. Lett. **84**, 20001 (2008).
[10] J. Cho, D. G. Angelakis, and S. Bose, Phys. Rev. Lett. **101**, 246809 (2008).
[11] J. Koch, A. A. Houck, K. L. Hur, and S. M. Girvin, Phys. Rev. A **82**, 043811 (2010).
[12] M. Hafezi, E. A. Demler, M. D. Lukin, and J. M. Taylor, Nat. Phys. **7**, 907 (2011).
[13] L. Zhou, Z. R. Gong, Y. X. Liu, C. P. Sun, and F. Nori, Phys. Rev. Lett. **101**, 100501 (2008).
[14] Z. R. Gong, H. Ian, L. Zhou, and C. P. Sun, Phys. Rev. A **78**, 053806 (2008).
[15] D. Z. Xu, Y. Li, C. P. Sun, and P. Zhang, Phys. Rev. A **88**, 013832 (2013).
[16] L. Zhou, Y. Chang, H. Dong, L. M. Kuang, and C. P. Sun, Phys. Rev. A **85**, 013806 (2012).
[17] J. T. Shen and S. Fan, Phys. Rev. Lett. **95**, 213001 (2005).
[18] A. Wallraff, D. I. Schuster, A. Blais, L. Frunzio, R. S. Huang, J. Majer, S. Kumar, S. M. Girvin, and R. J. Schoelkopf, Nature (London) **431**, 162 (2004).
[19] M. Mariantoni, F. Deppe, A. Marx, R. Gross, F. K. Wilhelm, and E. Solano, Phys. Rev. B **78**, 104508 (2008).
[20] T. Niemczyk, F. Deppe, H. Huebl, E. P. Menzel, F. Hocke, M. J. Schwarz, J. J. Garcia-Ripoll, D. Zueco, T. Hümmer, E. Solano, A. Marx, and R. Gross, Nat. Phys. **6**, 772 (2010).